



저작자표시-비영리-변경금지 2.0 대한민국

이용자는 아래의 조건을 따르는 경우에 한하여 자유롭게

- 이 저작물을 복제, 배포, 전송, 전시, 공연 및 방송할 수 있습니다.

다음과 같은 조건을 따라야 합니다:



저작자표시. 귀하는 원저작자를 표시하여야 합니다.



비영리. 귀하는 이 저작물을 영리 목적으로 이용할 수 없습니다.



변경금지. 귀하는 이 저작물을 개작, 변형 또는 가공할 수 없습니다.

- 귀하는, 이 저작물의 재이용이나 배포의 경우, 이 저작물에 적용된 이용허락조건을 명확하게 나타내어야 합니다.
- 저작권자로부터 별도의 허가를 받으면 이러한 조건들은 적용되지 않습니다.

저작권법에 따른 이용자의 권리는 위의 내용에 의하여 영향을 받지 않습니다.

이것은 [이용허락규약\(Legal Code\)](#)을 이해하기 쉽게 요약한 것입니다.

[Disclaimer](#)

이학석사학위논문

Development of a Novel Drug
Carrier Using Cyclodextrins
Containing Maleic Anhydride
Moieties

2015년 2월

서울대학교 대학원
화학부 생화학 전공
박 으 품 (Euddeum Park)

Development of a Novel Drug Carrier Using Cyclodextrins Containing Maleic Anhydride Moieties

지도교수 이 연

이 논문을 이학석사학위논문으로 제출함

2015년 2월

서울대학교 대학원

화학부 생화학 전공

박 으 품 (Euddeum Park)

박 으 품 (Euddeum Park)의 석사학위논문을 인준함

2015년 2월

위 원 장 _____ (인)

부 위 원 장 _____ (인)

위 원 _____ (인)

Abstract

Development of a Novel Drug Carrier Using Cyclodextrins Containing Maleic Anhydride Moieties

박 으 품 (Euddeum Park)

Department of Chemistry

College of Natural Sciences

Seoul National University

I developed a new pH-sensitive drug delivery carrier based on β -cyclodextrin (β -CD) and 1-methyl-2-(20-carboxyethyl) maleic anhydrides (MCM). The primary hydroxyl groups of β -CD were successfully attached to MCM residues to produce a medusa-like β -CD-MCM. The MCM residue was conjugated with cephadrine (CP) with high efficiency (>90%). More importantly, β -CD-MCM-CP responded to the small pH drop from 7.4 to 5.5 and released greater than 80% of the drugs within 0.5 h at pH 5.5. In addition, the inclusion complex between β -CD-MCM-CP and the ada-

mantane derivative was formed by simple mixing to show the possibility of introducing multi-functionality. Based on these results, b-CD-MCM can target weakly acidic tissues or organelles, such as tumours, inflammatory tissues, abscesses or endosomes, and be easily modified with various functional moieties, such as ligands for cell binding or penetration, enabling more efficient and specific drug delivery.

Keyword: Acidic environment, cephradine, dimethylmaleic acid anhydride, drug conjugation.

Student number: 2012-20274

Contents

◆ Abstract

1. Introduction	6
2. Materials and Methods	10
3. Results	19
4. Discussion	24
5. Conclusion	29
6. References	30
7. Figures	36
◆ 국문 초록 (Abstract in Korean)	45

1. Introduction

For efficient and safe delivery of drugs to specific targets, smart drug delivery techniques have evolved along with the development of various signal-responsive materials [1-3].

Abrupt changes in the physicochemical properties of smart materials in response to physical signals such as temperature [4] and light [5] as well as chemical signals such as pH [6], glutathione [7], and enzymes [8] can induce encapsulation and release of drugs in specific conditions. Among these, pH has been frequently selected as the controlling trigger because the pH value can represent a certain physiological condition in many target sites in the body. The pH variation through the gastrointestinal tract has been used for the site-specific drug delivery to strongly acidic stomach or weakly alkaline small intestine [9]. Enhanced glycolysis in cancer tissues lowers the pH to 5-6, and similar pH lowering is also observed in inflammatory tissues [10] and abscesses [11,12]. The weakly acidic pH value is recognised as an inducing signal for the release of anti-cancer [13] or anti-inflammatory drugs [14]. Moreover, the early endosomal pH value of 5-6 is frequently used as the signal for the endosomal escape of macromolecular drugs such as pDNA [15], siRNA [16] or proteins [17], which have difficulty penetrating the cell membrane and should be delivered into the cell interior via an endocytic pathway [18]. However, smart materials with rapid degradability responding to small pH variations are still under active investigation for a more practical drug delivery system because the

pH variation in the human body is not extreme, with a few exceptions. As a chemical moiety for pH-responsive smart materials, maleic acid amide derivatives are attractive owing to their rapid degradability at an appropriate pH. Unlike other amides, which can only be degraded at extreme pH conditions, maleic acid amide derivatives can be degraded within a biologically tolerable pH range [19]. The responsive pH range and the degradation rate can be finely tuned by a change of alkyl substituents on the cis-double bonds [20]. Moreover, the maleic acid amide derivatives can be synthesised via the onestep ring-opening reaction between amines and corresponding maleic acid anhydride derivatives under weakly alkaline conditions. The easy synthesis of maleic acid amide derivatives under mild conditions is a strong advantage over other pH-sensitive linkages, which require quite complicated synthetic steps in conjugation of drugs or cross-linking of carrier backbones [21]. In this study, we wanted to synthesise a drug carrier based on 1-methyl-2-(20-carboxyethyl) maleic anhydride (MCM) or carboxylate dimethyl maleic anhydride (CDM), a maleic acid anhydride derivative with two alkyl substituents. Because the acid amide correspondent from MCM is stable at normal physiological pH 7.4 but rapidly degradable at pH 5.5 [22], an MCM derivative might be one of the best candidates for the conjugation with drugs targeting weakly acidic environments. We designed a drug carrier with several MCM residues on the surface for the easiest conjugation with aminebased drugs or cross-linkers. As the backbone of the drug carrier, we selected β -cyclodextrin (β -CD), a cyclic oligosaccharide with seven glucose molecules. β -Cyclodextrin (β -CD) has been widely

used as a part of drug delivery carrier due to its high biocompatibility [23]. Many functional groups can be readily introduced into the b-CD backbone because it has 7 primary and 14 secondary hydroxyl groups. A medusa-like structure can be synthesised by reaction with the seven primary hydroxyl groups [24]. The regioselective functionalization of b-CD enables to achieve homogeneous chemical properties of the conjugated functional moieties. Furthermore, the toroidal interior of b-CD can be used for the introduction of additional functionality such as a targeting ligand [25] or cellpenetrating moiety [26] by host-guest inclusion because the interior can strongly interact with small hydrophobic molecules such as adamantane via non-covalent interactions [27]. Polymers or nanoparticles with adamantane moieties can be easily modified with b-CD derivatives by the host-guest interaction [28]. We expected that the medusa-like b-CD could be conjugated with drug molecules via pH-sensitive MCM linkers by simple mixing in mildly alkaline conditions and that other functional moieties with adamantane residues could also be non-covalently introduced into the pore of the b-CD. Otherwise, the surface of other drug carriers such as polymers or nanoparticles can be non-covalently modified with the pH-sensitive medusa-like b-CD derivative. The resulting carrier could rapidly release the conjugated drugs in weakly acidic conditions. The general conceptual scheme is illustrated in Figure 1. By using cephadrine (CP), a cephalosporin antibiotic, as a drug to be targeted to weakly acidic inflammatory tissues, we wanted to prove our concept in vitro. The medusa-like b-CD derivatives has strong potential for multi-functional drug delivery systems for targeting

tumours, inflammatory tissues or abscesses as well as for the rapid response at the pH of early endosomes in intracellular drug delivery.

2. Materials and methods

2.1. Materials

CP was obtained from Han Wha Pharm. Co., Ltd. (Seoul, South Korea). β -CD, 6-aminohexanoic acid, di-tert-butyl dicarbonate ((Boc)₂O), n-butylamine (BA), triethylamine (TEA), diisopropylethylamine (DIPEA), diisopropylcarbodiimide (DIC), 4-dimethylaminopyridine (DMAP), p-toluenesulphonic acid (PTSA), trifluoroacetic acid (TFA), sodium hydride (NaH) (60% in mineral oil), N,N,N',N'-tetramethyl-O-(1H-benzotriazol-1-yl)uronium hexafluorophosphate (HBTU), fluorescein isothiocyanate (FITC) isomer I and dimethylsulphoxide (DMSO) were purchased from Sigma-Aldrich (St Louis, MO). Triethyl-2-phosphonopropionate, dimethyl-2-oxoglutarate and 1-adamantaneamine hydrochloride were purchased from TCI (Tokyo, Japan). Ammonium chloride (NH₄Cl), magnesium sulphate (MgSO₄), potassium hydroxide (KOH), sodium chloride (NaCl), sodium hydroxide (NaOH), sodium bicarbonate (NaHCO₃), tetrahydrofuran (THF), dimethylformamide (DMF), hexane, ethyl acetate (EA), methanol (MeOH), ethanol, dichloromethane (DCM), hydrochloric acid (HCl), acetonitrile (ACN) and pyridine were purchased from Daejung (Seoul, South Korea). Anhydrous TEA, THF and DMF were obtained by distillation of the reagent-grade materials. Other reagents were used without further purification.

2.2. Synthesis

Synthesis of compound 1.

Following the method described in a previous report [29], compound 1 was prepared. Briefly, NaH (0.37 g, 9.2 mmol) was added slowly into a solution of triethyl-2-phosphonopropionate (1.64 g, 6.89 mmol) in anhydrous THF (30 mL) at 0 °C under a nitrogen atmosphere. Dimethyl-2-oxoglutarate (1.00 g, 5.74 mmol) was added to the solution after the evolution of hydrogen gas had stopped. The reaction mixture was further stirred while maintaining the temperature at 0 °C. After the reaction completion was confirmed by TLC, a saturated aqueous solution of NH₄Cl was added dropwise. Following the removal of THF by rotary evaporation, the resulting solid and water mixture was extracted with EA several times. The organic phase was combined, washed with deionised water (DIW) and brine, dried over MgSO₄ and concentrated by rotary evaporation. The residue was purified by silica gel chromatography eluted with EA/hexane to yield compound 1 as a colourless oil. Yield: 91%, ¹H NMR (300 MHz, CDCl₃): δ 1.25-1.30 (3H, t, CH₃CH₂O), 1.98 (3H, s, CH₃C), 2.46-2.49 (2H, m, CCH₂CH₂), 2.62-2.65 (2H, m, CH₂CH₂CO), 3.66 (3H, s, CO₂CH₃), 3.73 (3H, s, CH₃O₂CC) and 4.16-4.22 (2H, q, CH₃CH₂O).

Synthesis of compound 2.

Following the method described in a previous report [29], compound 2 was prepared. Briefly, compound 1 in a 2M KOH solution in ethanol was allowed to reflux for 1 h. DIW was added, and the hot reaction mixture was cooled to ambient temperature. After removal of ethanol by evaporation, the aqueous phase was washed with DCM several times and acidified to pH 2 using concentrated HCl. The aqueous phase was then extracted with EA several times. The organic phase was dried over MgSO₄ and concentrated un

der reduced pressure to produce MCM (2) as a white solid.

Yield: 74%, ^1H NMR (300 MHz, CDCl_3): d 2.12 (3H, s, CCH_3) and 2.77 (4H, s, $\text{CCH}_2\text{CH}_2\text{CO}$).

Synthesis of compound 3.

To a solution of compound 2 (2.00 g, 1.09 mmol), b-CD (0.10 g, 0.092 mmol), DMAP (0.46 g, 0.37 mmol) and PTSA (0.70 g, 0.37 mmol) in DMF (10 mL) was added DIC (0.33 g, 2.6 mmol). The reaction mixture was stirred overnight at ambient temperature. The crude product was purified by dialysis with regenerated cellulose membrane (MWCO 1000, SPECTRUM) in phosphate buffer (pH 9.0), HCl solution (pH 3.0) and DIW, respectively. Lyophilisation was performed next. An off-white powder, b-CD-MCM (3) was obtained. Yield: 85%, ^1H NMR (300 MHz, 1.1 wt% NaOD in D_2O): d 1.65 (3H, s, CCH_3), 1.98-2.10 (2H, m, CCH_2CH_2), 2.21-2.33 (2H, m, $\text{CH}_2\text{CH}_2\text{CO}$), 3.26-3.36 (2H, m, 20, 40-CH-b-CD), 3.67-3.80 (4H, m, 30, 50-CH, 60- CH_2 -b-CD), 4.94 (1H, s, 10-CH-b-CD) (Figure 3a); matrix-assisted laser desorption ionization-time of flight (MALDI-TOF) (m/z): 1490, 1656, 1882, 1988, 2155 and 2321 $[\text{M}+\text{Na}]^+$ (Figure 3b).

Synthesis of compound 4.

A solution of 3 (0.050 g, 0.024 mmol) in ACN (5 mL) was added with excess TEA at ambient temperature and stirred until becoming a completely clear solution. BA (0.24 mL, 0.242 mmol) was added dropwise into the reaction mixture. After overnight stirring, the reaction mixture was evaporated to remove the solvents. A 1M NaOH solution (12 equiv.) was added carefully to the aqueous solution of compound 4 to exchange excess n-butylammonium cations with sodium cations. The aqueous crude was evaporated and dried in vacuum, and then a light brown powder, b-CD-MCM-BA (4),

was obtained. Yield: 490%, ^1H NMR (300 MHz, 1.1 wt% NaOD in D_2O): d 0.89-0.94 (3H, t, CH_3CH_2), 1.32-1.39 (2H, m, $\text{CH}_3\text{CH}_2\text{CH}_2$), 1.46-1.54 (2H, m, $\text{CH}_2\text{CH}_2\text{CH}_2$), 1.87 (3H, s, CCH_3), 2.22- 2.31 (2H, m, $\text{CH}_2\text{CH}_3\text{CO}$), 2.49-2.56 (2H, m, CCH_2CH_2), 3.18-3.23 (2H, m, $\text{CH}_2\text{CH}_2\text{NH}$), 3.54-3.63 (2H, m, 20, 40-CH-b-CD), 3.65-3.92 (4H, m, 30, 50-CH, 60- CH_2 -b-CD), 5.05 (1H, s, 1H, s, 10-CH-b-CD).

Synthesis of compound 5.

b-CD-MCM-CP (5) was synthesised employing the same preparati on method as used for compound 4, but using CP solution (6 eq uiv.) in ACN instead of BA. After purification, yellow solid was ob tained. Yield:490%, ^1H NMR (300 MHz, 1.1 wt% NaOD in D_2O): d1. 83 (3H, s, CH_3 -cephalosporin), 1.86 (3H, s, CCH_3), 2.18-2.24 (2H, m, CCH_2H_2), 2.45-2.48 (2H, m, $\text{CH}_2\text{CH}_2\text{CO}$), 2.62-2.71 (4H, m, 30, 6 0- CH_2 -cyclohexadiene), 2.99-3.08 (1H, m, SCH_2C -cephalosporin), 3.12-3.18 (1H, m, SCH_2C cephalosporin), 3.39-3.49 (2H, m, 20, 40- CH-b-CD), 3.77-3.83 (4H, m, 30, 50-CH, 60- CH_2 -b-CD), 4.73 (1H, s, 10-CCHcyclohexadiene), 4.87 (1H, s, NCHS), 4.90 (1H, s, 10-CH b-CD), 5.71-5.73 (3H, m, NHCHCO , 40, 50-CH-cyclohexadiene), 5.8 7 (1H, s, 20-CH-cyclohexadiene).

Synthesis of compound 6.

6-Aminohexanoic acid (1.00 g, 7.26 mmol) was dissolved in the c o-solvent of THF:aqueous saturated NaHCO_3 solution (1:1) and a solution of ditert-butyl dicarbonate (2.00 g, 9.15 mmol) in THF w as added dropwise into the solution at ambient temperature. Afte r the reaction completion was confirmed by TLC, following the re moval of THF by rotary evaporation and the resulting solution w as acidified down to pH 1-2. The mixture was extracted with DC M several times. The organic phase was combined, washed with d

eionised brine, dried over MgSO_4 and concentrated by rotary evaporation. The pure compound, N-Boc-aminohexanoic acid (6) was obtained as an opaque crystal. Yield: 81%, ^1H NMR (300 MHz, 1.1 wt% NaOD in D_2O): δ 1.10-1.28 (2H, m, $\text{CH}_2\text{CH}_2\text{CH}_2$), 1.32-1.56 (13 H, m, $\text{CH}_2\text{CH}_2\text{CH}_2\text{CH}_2\text{CH}_2$, t-Boc), 2.10-2.15 (2H, t, $\text{CH}_2\text{CH}_2\text{CO}_2\text{H}$) and δ 2.99-3.03 (2H, t, NHCH_2CH_2).

Synthesis of compound 7.

Following the method described in a previous report [30], compound 7 was prepared. Briefly, a solution of compound 6 (0.10 g, 0.43 mmol) and 1-adamantaneamine hydrochloride (0.080 g, 0.43 mmol) in dry THF (9 mL) was treated with DIPEA (0.12 mL, 0.86 mmol) and HBTU (0.16 g, 0.43 mmol). After being stirred for 16 h at room temperature, the reaction mixture was heated at 60 °C for 90 min. Then, DCM and brine were added, and the organic phase was washed twice with 1M aqueous HCl (10 mL), twice with 5% aqueous NaHCO_3 (10 mL) and twice with brine (10 mL), and then dried over Na_2SO_4 . The residue was purified by silica gel chromatography eluted with EA/hexane to yield compound 7 as a white solid. Yield: 54%, ^1H NMR (300 MHz, CDCl_3): δ 1.27-1.35 (2H, m, $\text{CH}_2\text{CH}_2\text{CH}_2$), 1.42-1.49 (11H, s, m, t-Boc, $\text{CH}_2\text{CH}_2\text{CO}$), 1.55-1.59 (2H, m, NHCH_2CH_2), 1.61-1.65 (6H, br, $\text{CCH}_2\text{CH-ADM}$), 1.89-1.97 (6H, br, $\text{CHCH}_2\text{CH-ADM}$), 2.03-2.08 (5H, m, $\text{CH}_2\text{CHCH}_2\text{-ADM}$, $\text{CH}_2\text{CH}_2\text{CO}$) and 3.08-3.14 (2H, m, NHCH_2CH_2).

Synthesis of compound 8.

Excess TFA (10 mL) was added to compound 7 (0.75 g, 2.1 mmol) in DCM (30 mL) at 0°C. The solution was stirred for 2 h, concentrated, washed with saturated NaHCO_3 and brine, and dried over MgSO_4 . Compound 8 was obtained as a white solid without further

r purification. Yield: 89%, ^1H NMR (300 MHz, 1.2 wt% DCl in D_2O): d 1.16–1.26 (2H, m, $\text{CH}_2\text{CH}_2\text{CH}_2$), 1.40–1.56 (10H, m, $\text{CH}_2\text{CH}_2\text{CH}_2$, C $\text{CH}_2\text{CH-ADM}$), 1.81 (6H, br, $\text{CHCH}_2\text{CHADM}$), 1.89 (3H, br, $\text{CH}_2\text{CHCH}_2\text{-ADM}$), 2.04–2.09 (2H, t, $\text{CH}_2\text{CH}_2\text{CO}$) and 2.80–2.85 (2H, t, $\text{NH}_2\text{CH}_2\text{CH}_2$).

Synthesis of compound 9.

FITC isomer 1 (0.04 mg, 0.113 mmol) was added in a solution of compound 8 (0.030 g, 0.11 mmol) in MeOH (5 mL), followed by saturated NaHCO_3 (1 mL). After stirring overnight, the reaction mixture was purified by reverse-phase high-performance liquid chromatography (HPLC) with a linear gradient over 30 min from 50 to 100% of ACN/DIW with 0.1% TFA at a flow rate of 6 mL/min. Compound 9 was obtained as an orange solid. Yield: 32%, ^1H NMR (300 MHz, MeOD): d 1.40–1.45 (2H, m, $\text{CH}_2\text{CH}_2\text{CH}_2$), 1.61–1.66 (2H, m, $\text{CH}_2\text{CH}_2\text{CO}$), 1.69–1.73 (8H, s, m, $\text{CCH}_2\text{CH-ADM}$, NHCH_2CH_2), 2.01 (9H, br, $\text{CHCH}_2\text{CH-ADM}$, $\text{CH}_2\text{CHCH}_2\text{-ADM}$), 2.13–2.16 (2H, t, $\text{CH}_2\text{CH}_2\text{CO}$), 3.65 (2H, br, NHCH_2CH_2), 6.55 (2H, s, 20-CH-xanthene), 6.56–6.58 (2H, dd, 40-CH-xanthene), 7.17–7.19 (2H, d, 50-CH-xanthene), 7.20–7.22 (1H, d, 40-CH-isobenzofuranone), 7.62–7.64 (1H, d, 50-CH-isobenzofuranone), 7.82 (1H, s, 70-CH-isobenzofuranone).

2.3. Measurement of pH-sensitive drug release

Release of BA from b-CD-MCM-BA pH-sensitive release of BA from b-CD-MCM-BA (4) was confirmed by ^1H NMR. b-CD-MCM-BA was dissolved in 1.2 wt% DCl at the concentration of 3 mg/mL. After incubation with stirring at 37°C for 8 h, ^1H NMR was measured by a Bruker Avance DPX-300 (Germany) (Figure 4). Release of CP from b-CD-MCM-CP b-CD-MCM-CP (5) was

dissolved in a pH 7.4 phosphate buffer (100 mM) or a pH 5.5 acetate buffer (100mM) at a concentration of 3 mg/mL, and each solution was incubated with stirring at 37°C. A YOUNGLIN HPLC (9000 HPLC, South Korea) equipped with a UV detector and a reversephase column (Agilent Eclipse XDB-C18 4.6150 mm, 5 mm) was used for the HPLC-based measurement. At various time points, each sample was collected and diluted 10 times with the same buffer. After filtering through a 0.2- μ m polyvinylidene fluoride syringe filter, the sample was injected into the HPLC system. A mixture (3:7 v/v) of MeOH:pH 9.0 phosphate buffer (50mM) was used as the eluent, and the flow rate was set at 0.5 mL/min. The release of CP was measured by UV absorbance at wavelengths 245 and 270 nm (Figure 5).

2.4. Complex formation between compound 5 and 9

Fluorescence correlation spectroscopy measurement A home-built fluorescence confocal microscope setup was used to measure the autocorrelation of the fluorescent probe, FITC. A 488-nm continuous blue laser diode (TECBL-20GC-488, World Star Tech, Toronto, Canada) was coupled with a single-mode optical fibre ($\Phi=3-5 \mu\text{m}$, P1-488-PM-FC, Thorlabs, Newton, NJ) for the beam clean-up and illuminated the sample through a water-immersion objective (NA=1.20, 60X, f=3 mm, Olympus, Tokyo, Japan) mounted in a homemade microscope body. The fluorescence signal was distinguished with the excitation light by a dichroic mirror (ZT488rdc, Chroma, Bellows Falls, VT) and further cleaned by an emission filter (HQ525/50 m, Chroma). A 1:2 multimode fibre optic coupler ($\Phi=62.5 \mu\text{m}$, FCMM625-50A-FC) was

used as a pinhole to reduce the background from the focal volume, and two avalanche photodiodes (SPCM-AQR-14-FC, Perkin Elmer, Waltham, MA) collected the fluorescence signals. The correlation was measured with a correlator card (FLEX02-01D, Correlator.com) and further analysed by a homemade analysis program coded with LabVIEW 2009 (National Instruments, Austin, TX). The fluorescence correlation spectroscopy (FCS) setup was calibrated to determine the axial and lateral dimensions of the confocal volume by using a fluorophore, Alexa 488, whose diffusion coefficient is $D=4.35106 \times 10^{-6} \text{cm}^2/\text{s}$ [31]. The process followed the procedure described in reference [32]. Calibration showed that the lateral $1/e^2$ dimension was 232 nm with the aspect ratio of 7.18, indicating that the measured focal volume was 0.501 fL. For the measurement of complex formation, a solution of compound 9 (10 nM) in pH 9.0 phosphate buffer (50 mM) was prepared with different concentrations of compound 5. Bovine serum albumin was added to the mixture at the final concentration of 0.1 mg/mL to prevent the nonspecific binding between compounds 5 and 9. Each correlation curve was measured six times for 10 min each (once for each concentration of compound 5) to suppress the thermal noises and background signals. Rotating frame overhauser effect spectroscopy The complex between b-CD and compound 9 and the complex between b-CD-MCM-CP (compound 5) and compound 9 were prepared by mixing at a 1:1 molar ratio at a concentration of 3mM in a D2O-based pH 9.0 phosphate buffer (50 mM). NMR spectra recorded at 25°C on a Agilent Technologies 400-MR DD2 (Santa Clara, CA) spectrometer. Rotating frame overhauser effect spectroscopy (ROESY) experi-

ment was performed using the standard protocols contained in the spectrometer library (mixing time: 300 ms; T₁ experiment).

2.5. Cytotoxicity

Cell viability was measured by 3-(4,5-dimethylthiazol-2-yl)-2,5-diphenyltetrazolium bromide (MTT; Sigma-Aldrich) assay. NIH-3T3 cells (mouse embryonic fibroblast cell line) were seeded at 5.0103 cells/well in a 96-well plate in 90 μ L of Dulbecco's modified eagle's medium WelGene containing 10% foetal bovine serum; WelGene (Daegu, South Korea) and incubated at 37°C for 24 h. To determine the cytotoxicity, 10 μ L of the solution of each sample with various concentrations was added into the media with subsequent incubation at 37°C for 48 h. For the assay, the cells were washed with Dulbecco's phosphate-buffered saline (DPBS; WelGene), followed by the addition of 20 μ L of filtered MTT solution (2 mg/mL in DPBS). After incubation at 37 °C for 2 h, the medium was removed from the well, and 150 μ L of DMSO was added to dissolve the insoluble formazan particles. The absorbance was measured at 570 nm using a microplate reader (Molecular Devices Co., Menlo Park, CA). The relative cell viability (%) was defined as the percentage of viable cells compared with the same percentage in the control (cells treated with DPBS solution).

3. Results

3.1. Synthesis of b-CD-MCM

We synthesised a pH-sensitive drug carrier based on b-CD and MCM for efficient drug conjugation, rapid drug release at acidic pH and simple introduction of functional ligands. The synthetic scheme is shown in Figure 2(a). After the synthesis of MCM by the Horner-Wadsworth-Emmons reaction between triethyl-2-phosphonopropionate and dimethyl-2-oxoglutarate (Figure 2b) [29], MCM was coupled with the b-CD molecule via the formation of ester bond between the carboxyl group of MCM and the hydroxyl group of b-CD. A b-CD molecule has seven primary hydroxyl groups and fourteen secondary hydroxyl groups. Among them, primary hydroxyl groups at the 6-O position of the glucose are more reactive to electrophiles, and they preferably react with the carboxyl group using a carbodiimide-coupling reagent, DIC. b-CD-MCM was purified from the excess reagents by dialysis. The formation of b-CD-MCM was confirmed by ¹H NMR and MALDI-TOF mass spectrometry (Figure 3). The numbers of MCM residues per a b-CD-MCM molecule was calculated to be six by ¹H NMR. In other words, 85% of primary hydroxyl groups of b-CD were conjugated with MCM on average. The MALDI-TOF mass spectra exhibited the presence of b-CD-MCM molecules with various numbers of MCM residues: b-CD-(MCM)₂ (1490), b-CD-(MCM)₃ (1656), b-CD-(MCM)₄ (1822), b-CD-(MCM)₅ (1988), b-CD-(MCM)₆ (2154) and b-CD-(MCM)₇ (2322). Considering the average conjugation number was six by ¹H NMR and the main

peak of the MALDI-TOF spectra was that of b-CD-(MCM)₄, the MALDI-TOF spectra could not represent the distribution of various b-CD-(MCM) molecules accurately, most likely due to the different ionisation degrees of the b-CD-(MCM) variants.

3.2. Drug conjugation with b-CD-MCM

At first, a simple primary amine, BA, was used as a model drug for the optimisation of the conjugation reaction. By simple mixing in a weakly basic condition, BA was successfully introduced into b-CD-MCM. The ¹H NMR spectrum shows the formation of the acid amide linkage between BA and b-CD-MCM (Figure 4). Greater than 90% of MCM moieties in b-CD-MCM were reacted with BA, and only a small amount of unreacted BA were remained. Then, CP, an amine-containing antibiotic drug, was conjugated with b-CD-MCM by a similar method. The formation of b-CD-MCM-CP was confirmed by both ¹H NMR and HPLC. The amount of CP with a strong UV absorption was easily analysed by a UV detector. High conjugation efficiency (92.5±2.5%) was observed in the formation of b-CD-MCM-CP. As we applied six equivalents of CP to b-CD-MCM with six MCM moieties, nearly exhaustive conjugation was accomplished by the simple mixing. In addition, the drug content in b-CD-MCM-CP was calculated to be 28±5.5% by comparing the mass of CP and the total mass of b-CD-MCM-CP with some residual sodium and TEA salts.

3.3. pH-sensitive drug release

The pH-sensitive degradation of the MCM acid amide bond was investigated by ^1H NMR. The methylene protons (marked with x) next to the nitrogen in the intact amide of b-CD-MCM-BA showed a peak at 3.18–3.23 ppm, while the peak (marked with *) was shifted to 2.55–2.62 ppm, equal to the methylene peak of free BA, in an acidic solution (1.2 wt% DCl in D_2O) (Figure 4). The chemical shift confirmed the degradation of the MCM acid amide and the release of conjugated BA. Cumulative release of CP from b-CD-MCM-CP at pH 5.5 and pH 7.4 was measured by HPLC to determine the degradation kinetics in more detail (Figure 5). At pH 7.4, less than 20% of CP was released from b-CD-MCM-CP, even after 5 h. On the other hand, a rapid burst of CP was observed at pH 5.5, and more than 80% of CP was released within 0.5 h. The release was almost completed at approximately 95% in 1 h. A dramatic difference in release kinetics was observed between pH 5.5 and pH 7.4. In addition, we confirmed the stability of CP during the conjugation and release procedure. The ^1H NMR spectrum of the CP released from b-CD-MCM-CP at pH 5.5 was identical to that of the initial CP (Figure 6a). The mass spectra of the two CPs obtained by electrospray ionisation were also identical (350.1 $[\text{M}+\text{H}]^+$ and 699.1 $[\text{M}+\text{M}]^+$, Figure 6b). Based on these data, we believe that CP was quite stable during the conjugation in mildly basic conditions and during the release in weakly acidic conditions.

3.4. Complex formation between b-CD-MCM-CP and the adamantane derivative

To clarify the formation of the complex between the b-CD based

drug conjugate and an adamantane derivative, we used FCS, which analyses the variation in the diffusion coefficient of a fluorophore attached to guest or host [33]. FITC was conjugated to the adamantane derivative [34] as a probe (FITC-hex-ADM) (Figure 2c). The average diffusion time of the fluorophore was measured with varying the concentration of the host molecule, b-CD-MCM-CP. As the concentration of b-CD-MCM-CP increased, the average diffusion time also decreased, confirming the molecular weight increase and the complex formation (Figure 7). From the graph, the binding constant between b-CD-MCM-CP and FITC-hex-ADM was calculated to be 1.49104 M⁻¹. Furthermore, 2D ROESY NMR experiment was performed to show the formation of the inclusion complex. Figure 8(a and b) exhibit the ROESY spectra of the b-CD/FITC-hex-ADM and b-CD-MCM-CP/FITC-hex-ADM mixtures, respectively. The a, b and g protons of the adamantane in FITC-hex-ADM showed strong cross-peaks by interaction with the H3, H5 and H6 protons in the cavity of native b-CD, and weaker crosspeaks by interaction with the H2 and H4 protons on the exterior of the b-CD cavity (Figure 8a). Similarly, the cross-peaks between the protons of the adamantane derivatives and b-CD-MCM-CP were also observed (Figure 8b). The spectra represent the spatial proximity at the 5 Å maximal limit among the protons of b-CD derivatives and the adamantane moiety. Both data strongly indicate complex formation between b-CD-MCM-CP and FITC-hex-ADM.

3.5. Cytotoxicity

The short-term biocompatibility of the b-CD-MCM drug carrier was preliminarily checked by MTT assay on NIH3T3 cells (Figure 9). Branched polyethylenimine 25 kDa, a wellknown polymeric drug delivery carrier with high cytotoxicity, was used as a positive control. Up to 100 μ M, b-CD, b-CD-MCM and b-CD-MCM-CP exhibited almost no cytotoxicity until 48 h.

4. Discussion

In this study, we intended to develop a pH-sensitive drug carrier that could sense the small pH drop from 7.4 to 5.5 and rapidly release the conjugated drug molecules. A backbone with many conjugating residues was preferred for high drug contents. In addition, various functions can be introduced by a simple method for a multi-role drug delivery carrier. We selected b-CD as the backbone of the carrier due to high biocompatibility [20], modifiability of many hydroxyl groups [24] and strong non-covalent complex formation with adamantane [27]. As a pH-sensitive linker, we selected a maleic acid amide derivative because it can be easily synthesised by the simple mixing between the corresponding anhydride and amine and it shows pH-dependent degradability. A maleic acid amide derivative has a cis- β -carboxylate group that can internally attack the carbonyl group of the amide via five-membered ring formation, and it shows much higher vulnerability than a simple amide [20,35]. The pH sensitivity is also dependent upon the alkyl substituent on the cis-double bond. Bulkier substituents can accelerate the internal attack of the β -carboxylate group to increase the degradability at weakly acidic pH [36]. Among various maleic acid amide derivatives, we selected the MCM acid amide because it showed rapid degradability at pH 5.5 owing to the methyl and carboxyethyl substituents [22,37,38]. We successfully synthesised b-CD-MCM via a one-step reaction by the carbodiimide coupling method using DIC (Figure 2) under catalysts of DMAP and PTSA. Although coupling

reactions of MCM using thionyl chloride (SOCl_2) or oxalyl chloride were reported previously [39], they showed significant side reactions in the coupling between b-CD and MCM, so we selected the DIC coupling method to achieve a high yield of the product. The addition of both DMAP and PTSA could facilitate the ester formation without the formation of side products including N-acylurea in polar solvents [40]. We could control the numbers of MCM residues that coupled to b-CD by adjusting the amount of reactants, and consequently obtain a “medusa-like” b-CD-MCM with six MCM residues on average, which was confirmed by ^1H NMR and mass spectroscopy (Figure 3). Because the face of the secondary hydroxyl groups in b-CD readily interacts with an adamantane guest molecule [41], the medusa-like structure by the modification of primary hydroxyl group would be preferred for the future inclusion of a functional moiety. We expected a high efficiency in the drug conjugation with b-CD-MCM because the anhydride group of MCM is very reactive with nucleophiles such as primary amines in alkaline conditions, even if the nucleophilic attack is interfered with by steric hindrance. In both cases of b-CD-MCM-BA and b-CD-MCM-CP, we similarly observed high drug efficiency, with the values of 90% and 92.5% for BA and CP, respectively. By the covalent conjugation with b-CD-MCM, the drugs can avoid premature release from the drug delivery carrier in the diluted concentrations in physiological fluids. We investigated the drug-release kinetics of b-CD-MCM-CP at pH 5.5 and pH 7.4. Remarkably, CP was dramatically released from b-CD-MCM at pH 5.5 up to 80% within 0.5 h and 95% within 1 h, while it was barely released at pH 7.4 (Figure 5). The chemical

stability of CP during the conjugation and release was also secured. On the basis of the delicate sensing of the small pH difference and the outstanding release kinetics at the weakly acidic pH, we believe that b-CD-MCM can be used as a drug carrier for targeting tumours, inflammatory tissues or abscesses as well as for early endosomal escape in intracellular drug delivery. b-CD-MCM-CP enables the delivery of antibiotics into pneumonia or other inflamed tissues specifically, to avoid side effects and overdoses. As mentioned above, b-CD is a cyclic oligosaccharide composed of seven-membered α -D-glucopyranoside units linked 1 to 4, and it contains a less hydrophilic interior space and a more hydrophilic outer surface. This allows b-CD to form inclusion complexes with various molecules through host-guest interactions. Adamantane, a cycloalkane consisting of four connected cyclohexane rings, is the most representative guest molecule for b-CD. Therefore, we can introduce a functional moiety such as a targeting ligand or a cell penetrating peptide into b-CD-MCM by the tethering of an adamantane residue in the functional moiety and the simple mixing with b-CD-MCM. For the confirmation of this concept, we synthesised a FITC-labelled adamantane derivative to trace the inclusion complex by FCS. The diffusion coefficient of the fluorophore was decreased significantly due to the complex formation. The binding constant was calculated from the “S”-type curve between the diffusion time and the concentration of b-CD-MCM (Figure 7). The binding constant K was 1.49104 M⁻¹, meaning the interaction between b-CD-MCM-CP and the adamantane derivative was similar to the general b-CD/adamantane host-guest interaction because the

general association constant K is $1-10104 \text{ M}^{-1}$ [42]. Based on the binding constant, the inclusion percentage could also be calculated and be shown in Figure 7. The host-guest inclusion between b-CD-MCM-CP and adamantane derivative was further confirmed by ROESY spectra (Figure 8). Strong cross-peaks in b-CD-MCM-CP/FITC-hex-ADM were comparable with those of b-CD/FITChex-ADM. The medusa-like conjugation of six MCM molecules in the face of primary hydroxyl groups did not affect the inclusion significantly. Based on these results, any functional moieties could be introduced into b-CD-MCM after the drug conjugation by the formation of the inclusion complex. Of course, other drug carriers such as polymers or nanoparticles with adamantane moieties can be easily modified with b-CD-MCM through the host-guest interaction for pH-sensitive conjugation of drugs or other functionalities. Finally, we verified that b-CD-MCM and its drug conjugate showed almost no sign of acute cytotoxicity up to $100 \text{ } \mu\text{M}$ in a eukaryotic cell line by MTT assay (Figure 9), although the long-term toxicity and biadaptability should be analysed by various methods in the future. As a novel drug-conjugating system, b-CD-MCM has great advantages in easy conjugation of drugs and multifunctionalities as well as rapid release of drugs responding to small pH drop. CP, an antibiotic model drug in this research, can be specifically delivered into bacteria-infected sites by a b-CD-MCM-based drug carrier. b-CD-MCM, with a molar mass of several thousands, can be used as a pH-sensitive drug carrier by itself for a site-specific delivery of drugs into weakly acidic targets such as tumours, abscesses or inflammatory tissues. For longer circulation or enhanced perme-

ability and retention effect, b-CD-MCM can be introduced into other drug delivery carriers with several hundred nanometres by non-covalent interactions. The future animal study will be followed for the proof of the specificity and efficacy of b-CD-MCM-based drug delivery systems.

5. Conclusion

We successfully developed a novel drug delivery carrier, β -CD-MCM, which has a rapid release profile in response to a small pH drop. β -CD-MCM possesses several ready-to-use anhydride residues for simple and almost exhaustive conjugation with amine-containing drugs. β -CD-MCM-CP, one of the drug conjugates, exhibited a remarkable capability to discriminate between pH 7.4 and 5.5 to release the conjugate antibiotic. Moreover, the internal cavity of β -CD-MCM-CP is easily accessible for complexation with other functional groups with an adamantane residue. Based on these attractive characteristics, β -CD-MCM has great potential as a multifunctional drug delivery carrier for targeting tissues or organelles with weakly acidic pH conditions.

6. References

- [1]. Fleige E, Quadir MA, Haag R. Stimuli-responsive polymeric nanocarriers for the controlled transport of active compounds: concepts and applications. *Adv Drug Delivery Rev* 2012;64: 866-84.
- [2]. Lee Y, Kataoka K. Biosignal-sensitive polyion complex micelles for the delivery of biopharmaceuticals. *Soft Matter* 2009;5: 3810-17.
- [3]. Gupta P, Vermani K, Garg S. Hydrogels: from controlled release to pH-responsive drug delivery. *Drug Discovery Today* 2002;7: 569-79.
- [4]. Prasannan A, Tsai H-C, Chen Y-S, Hsiue G-H. A thermally triggered in situ hydrogel from poly(acrylic acid-co-N-isopropylacrylamide) for controlled release of anti-glaucoma drugs. *J Mater Chem B* 2014;2:1988-97.
- [5]. Jiang J, Tong X, Zhao Y. A new design for light-breakable polymer micelles. *J Am Chem Soc* 2005;127:8290-1.
- [6]. Lee Y, Fukushima S, Bae Y, et al. A protein nanocarrier from charge-conversion polymer in response to endosomal pH. *J Am Chem Soc* 2007;129:5362-3.
- [7]. Cheng R, Feng F, Meng F, et al. Glutathione-responsive nanovehicles as a promising platform for targeted intracellular drug and gene delivery. *J Controlled Release* 2011;152:2-12.
- [8]. Miyata T, Uragami T, Nakamae K. Biomolecule-sensitive

- hydrogels. *Adv Drug Delivery Rev* 2002;54:79-98.
- [9]. Gao W-W, Chan JM, Farokhzad OC. pH-responsive nanoparticles for drug delivery. *Mol Pharmaceutics* 2010;7:1913-20.
- [10]. Wu XL, Kim JH, Koo H, et al. Tumor-targeting peptide conjugated pH-responsive micelles as a potential drug carrier for cancer therapy. *Bioconjugate Chem* 2010;21:208-13.
- [11]. Punnia-Moorthy A. Evaluation of pH changes in inflammation of the subcutaneous air pouch lining in the rat, induced by carrageenan, dextran and *Staphylococcus aureus*. *J Oral Pathol Med* 1987;16:36-44.
- [12]. Bessman AN, Page J, Thomas LJ. In vivo pH of induced soft-tissue abscesses in diabetic and nondiabetic mice. *Diabetes* 1989;38: 659-62.
- [13]. Ford C, Hamel J, Stapert D, Yancey R. Establishment of an experimental model of a *Staphylococcus aureus* abscess in mice by use of dextran and gelatin microcarriers. *J Med Microbiol* 1989;28: 259-66.
- [14]. Abhay A, Singh CA, Vamanrao DP, Kumar JN. Poly(amidoamine) (PAMAM) dendritic nanostructures for controlled site-specific delivery of acidic anti-inflammatory active ingredient. *AAPS PharmSciTech* 2005;6:E536-42.
- [15]. Lee Y, Miyata K, Oba M, et al. Charge-conversion ternary polyplex with endosome disruption moiety: a technique for efficient and safe gene delivery. *Angew Chem Int Ed* 2008;47:5163-6.
- [16]. Rozema DB, Lewis DL, Wakefield DH, et al. Dynamic

- PolyConjugates for targeted in vivo delivery of siRNA to hepatocytes. *PNAS* 2007;104:12982-7.
- [17]. Lee Y, Ishii T, Cabral H, et al. Charge-conversional polyionic complex micelles-efficient nanocarriers for protein delivery into cytoplasm. *Angew Chem Int Ed* 2009;48:5309-12.
- [18]. Mellman I, Fuchs R, Helenius A. Acidification of the endocytic and exocytic pathways. *Annu Rev Biochem* 1986;55:663-700.
- [19]. Lee Y, Ishii T, Kim HJ, et al. Efficient delivery of bioactive antibodies into the cytoplasm of living cells by chargeconversional polyion complex micelles. *Angew Chem Int Ed* 2010;49:2552-5.
- [20]. Kirby AJ, Lloyd GJ. Structure and efficiency in intramolecular and enzymic catalysis: intramolecular general base catalysis. Catalysis of amide hydrolysis by the carboxy-group of substituted maleamic acids. *J Chem Soc Perkin Trans 2* 1976:1753-61.
- [21]. Mehta NB, Phillips AP, Lui FF, Brooks RE. Maleamic and citraconamic acids, methyl esters, and imides. *J Org Chem* 1960;25: 1012-15.
- [22]. Rozema DB, Ekena K, Lewis DL, et al. Endosomolysis by masking of a membrane-active agent (EMMA) for cytoplasmic release of macromolecules. *Bioconjugate Chem* 2003;14:51-7.
- [23]. Davis ME, Brewster ME. Cyclodextrin-based pharmaceuticals: past, present and future. *Nat Rev Drug Discovery* 2004;3:1023-35.
- [24]. Cravotto G, Bicchi C, Tagliapietra S, et al. New chiral selectors: design and synthesis of 6-TBDMS-2,3-methyl beta-cyclodextrin 2-20 thioureido dimer and 6-TBDMS-2,3-methyl

- (or 2-methyl-3-acetyl) beta-cyclodextrin bearing an (R) Mosher acid moiety. *Chirality* 2004;16:526-33.
- [25]. Motoyama K, Onodera R, Okamatsu A, et al. Potential use of the complex of doxorubicin with folate-conjugated methyl-beta-cyclodextrin for tumor-selective cancer chemotherapy. *J Drug Targeting* 2014;22:211-19.
- [26]. Copolovici DM, Langel K, Eriste E, Langel U. Cell-penetrating peptides: design, synthesis, and applications. *ACS Nano* 2014;8:1972-94.
- [27]. Hakkarainen B, Fujita K, Immel S, et al. ¹H NMR studies on the hydrogen-bonding network in mono-altro-beta-cyclodextrin and its complex with adamantane-1-carboxylic acid. *Carbohydr Res* 2005; 340:1539-45.
- [28]. Kulkarni A, Deng W, Hyun SH, Thompson DH. Development of a low toxicity, effective pDNA vector based on noncovalent assembly of bioresponsive amino-beta-cyclodextrin:adamantane-poly(vinyl alcohol)-poly(ethylene glycol) transfection complexes. *Bioconjugate Chem* 2012;23:933-40.
- [29]. Naganawa A, Ichikawa Y, Isobe M. Synthetic studies on tautomycin. Synthesis of 2,3-disubstituted maleic anhydride segment. *Tetrahedron* 1994;50:8969-82.
- [30]. Humblet V, Misra P, Bhushan KR, et al. Multivalent scaffolds for affinity maturation of small molecule cell surface binders and their Application to Prostate Tumor Targeting. *J Med Chem* 2009;52: 544-50
- [31]. Petrasek Z, Schwille P. Precise measurement of diffusion coefficients using scanning fluorescence correlation spectroscopy.

- Biophys J 2008;94:1437-48.
- [32]. Kim SA, Heinze KG, Schwille P. Fluorescence correlation spectroscopy in living cells. *Nat Methods* 2007;4:963-73.
- [33]. Granadero D, Bordello J, Perez-Alvite MJ, et al. Host-guest complexation studied by fluorescence correlation spectroscopy: adamantane-cyclodextrin inclusion. *Int J Mol Sci* 2010;11:173-88.
- [34]. Smirnov D, Dhall A, Sivanesam K, et al. Fluorescent probes reveal a minimal ligase recognition motif in the prokaryotic ubiquitin-like protein from *Mycobacterium tuberculosis*. *J Am Chem Soc* 2013; 135:2887-90.
- [35]. Suh J, Baek D-J. Intramolecular catalysis of amide hydrolysis by carboxyl and metal ion/proton agents. I. Intramolecular reactions of imidazole or pyridine derivatives of maleamic acid. *Bioorg Chem* 1981;10:266-76.
- [36]. Kirby AJ, McDonald RS, Smith CR. Intramolecular catalysis of amide hydrolysis by two carboxy groups. *J Chem Soc Perkin Trans 2* 1974:1495-504.
- [37]. Monahan SD, Subbotin VM, Budker VG, et al. Rapidly reversible hydrophobization: an approach to high first-pass drug extraction. *Chem Biol* 2007;14:1065-77.
- [38]. Takemoto H, Miyata K, Hattori S, et al. Acidic pH-responsive siRNA conjugate for reversible carrier stability and accelerated endosomal escape with reduced IFN α -associated immune response. *Angew Chem Int Ed* 2013;52:6218-21.
- [39]. Wong SC, Wakefield D, Klein J, et al. Hepatocyte targeting of nucleic acid complexes and liposomes by a T7 phage p17 peptide. *Mol Pharmaceutics* 2006;3:386-97.
- [40]. Moore JS, Stupp SI. Room temperature polyesterification.

Macromolecules 1990:23:65-70.

[41]. Li L, Guo X, Wang J, et al. Polymer networks assembled by hostguest inclusion between adamantyl and β -cyclodextrin substituents on poly(acrylic acid) in aqueous solution.

Macromolecules 2008; 41:8677-81.

[42]. Harries D, Rau DC, Parsegian VA. Solutes probe hydration in specific association of cyclodextrin and adamantane. J Am Chem Soc 2005:127:2184-90.

7. Figures

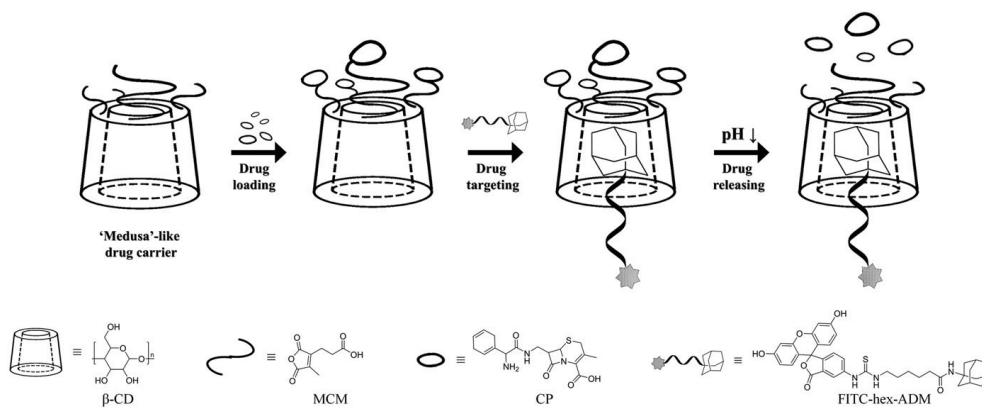


Figure 1. General scheme of pH-sensitive drug delivery by a medusa-like β -CD-MCM.

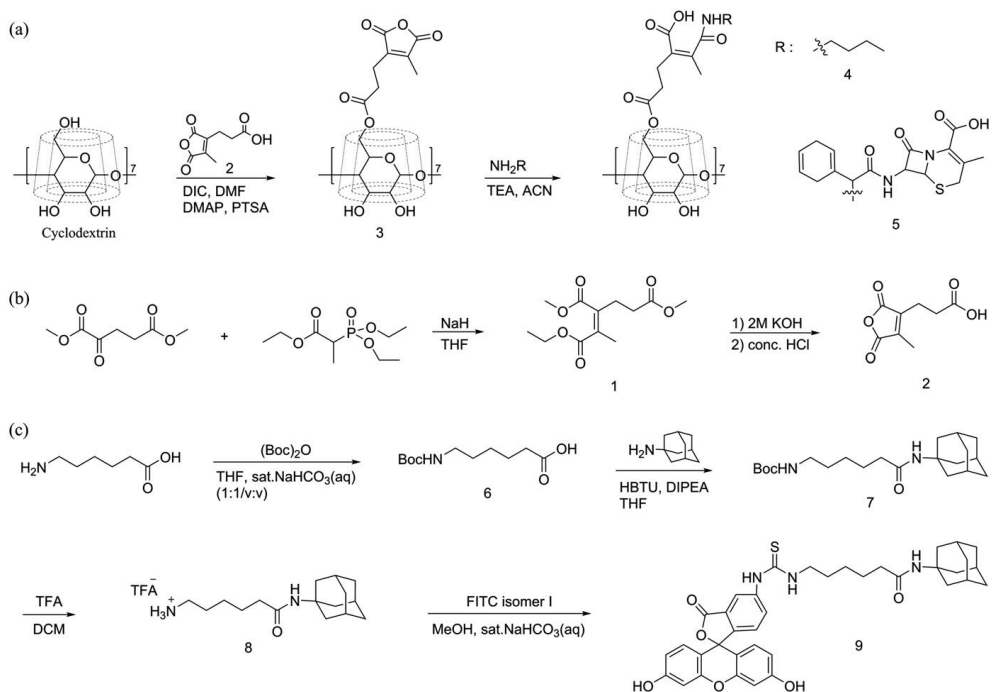


Figure 2. Synthetic schemes of β -CD-MCM and its drug conjugate. (a) Synthesis of β -CD-MCM-BA and β -CD-MCM-CP, (b) Synthesis of 1-methyl-2-(20-carboxyethyl) maleic anhydride (MCM) and (c) synthesis of FITC-hex-ADM.

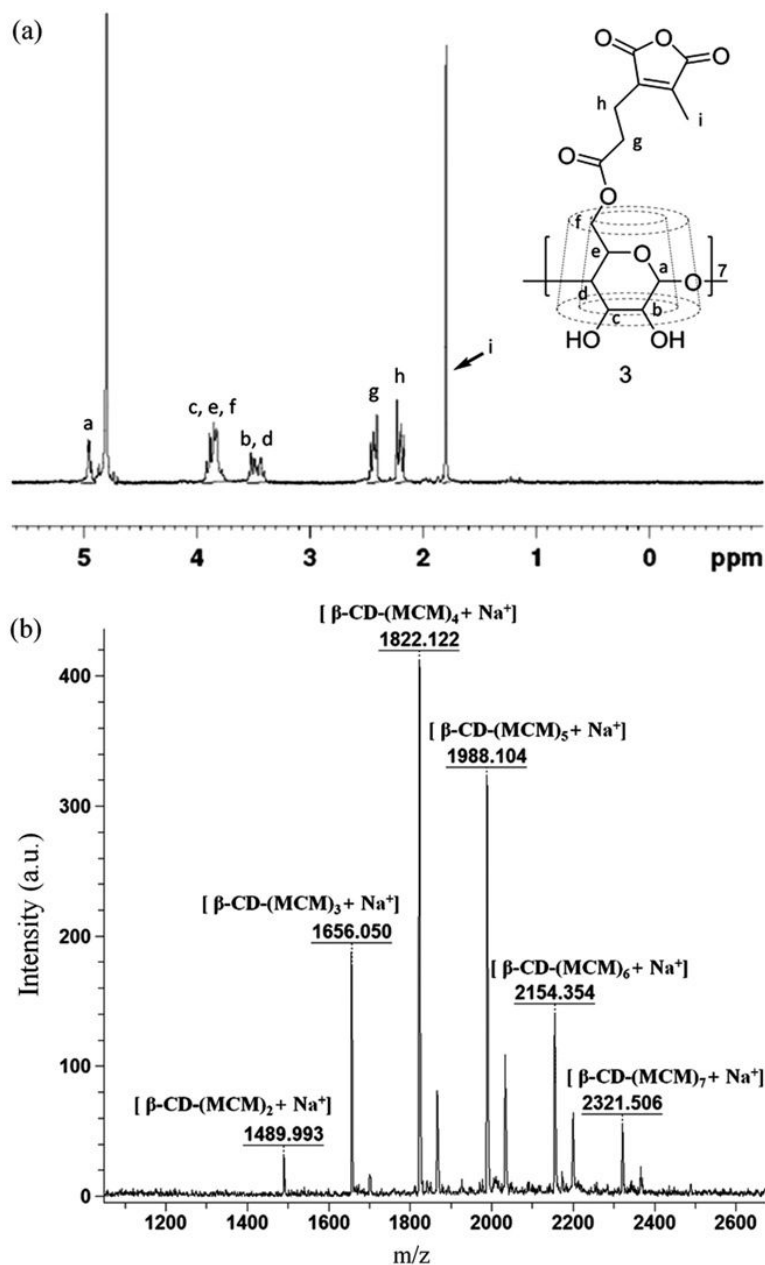


Figure 3. Confirmation of synthesis of $\beta\text{-CD-MCM}$. (a) ^1H NMR (NMR solvent: D_2O) and (b) MALDI-TOF spectra of $\beta\text{-CD-MCM}$.

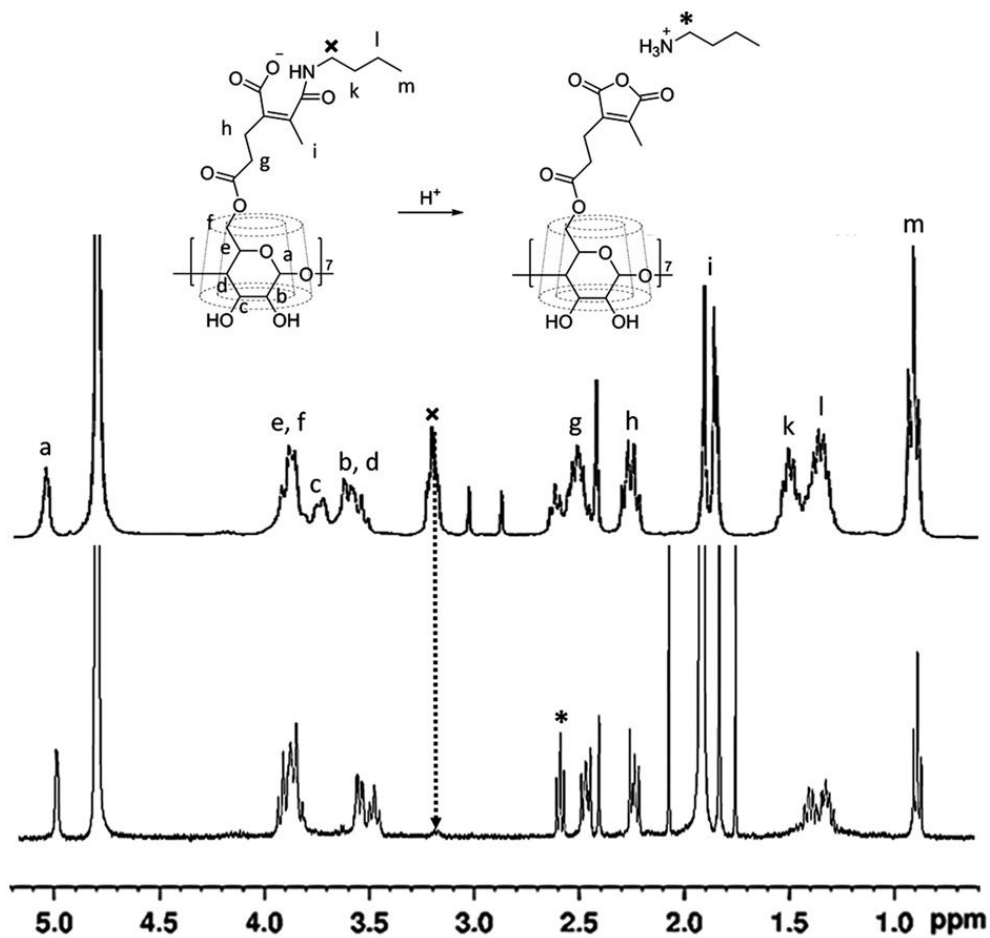


Figure 4. Release of BA from β -CD-MCM-BA at acidic pH measured by ^1H NMR (NMR solvent: D_2O).

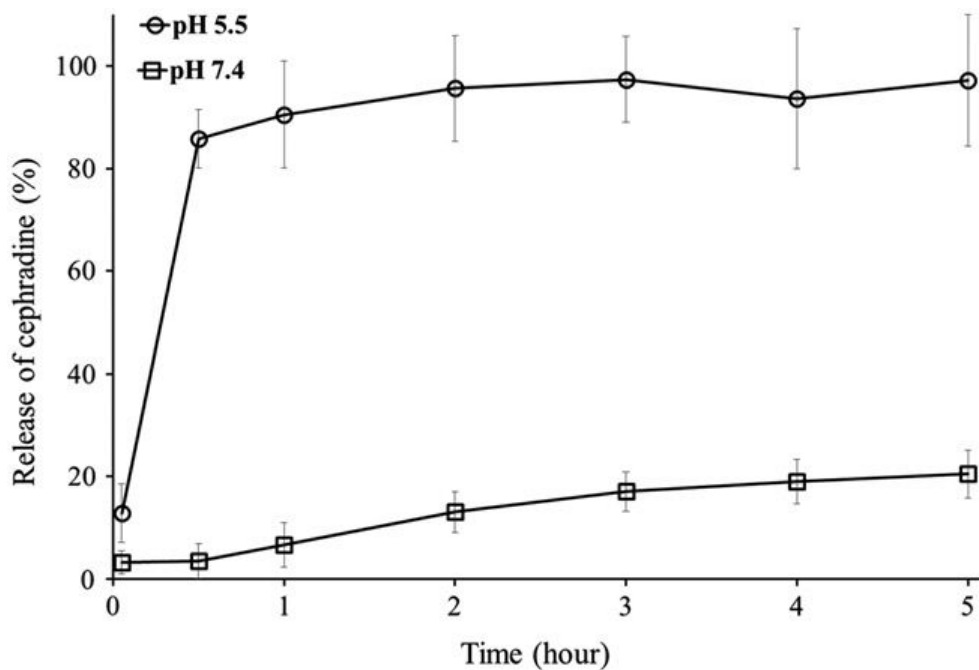


Fig. 5. pH-responsive release of CP from β -CD-MCM-CP at pH 5.5 (acetate buffer, 100mM; \circ) and pH 7.4 (phosphate buffer, 100 mM; \square) measured by HPLC. The error bar represents the standard deviation

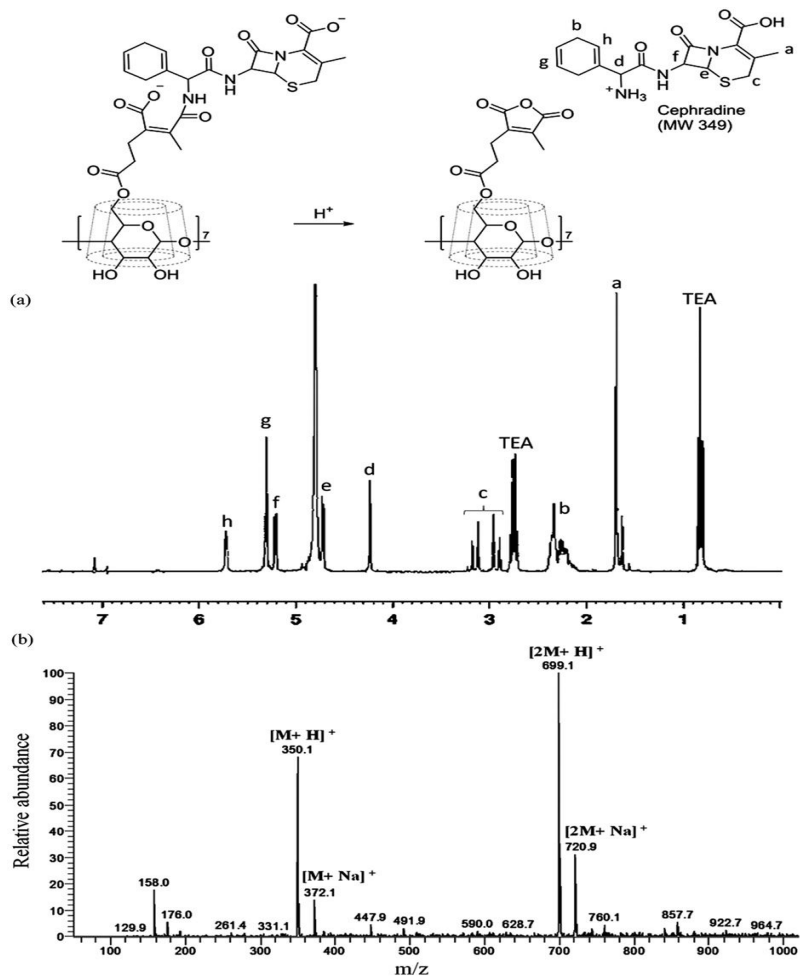


Figure 6. Identification of the released CP from β -CD-MCM-CP. (a) ^1H NMR (NMR solvent: D_2O) and (b) ESI mass spectra of the released CP.

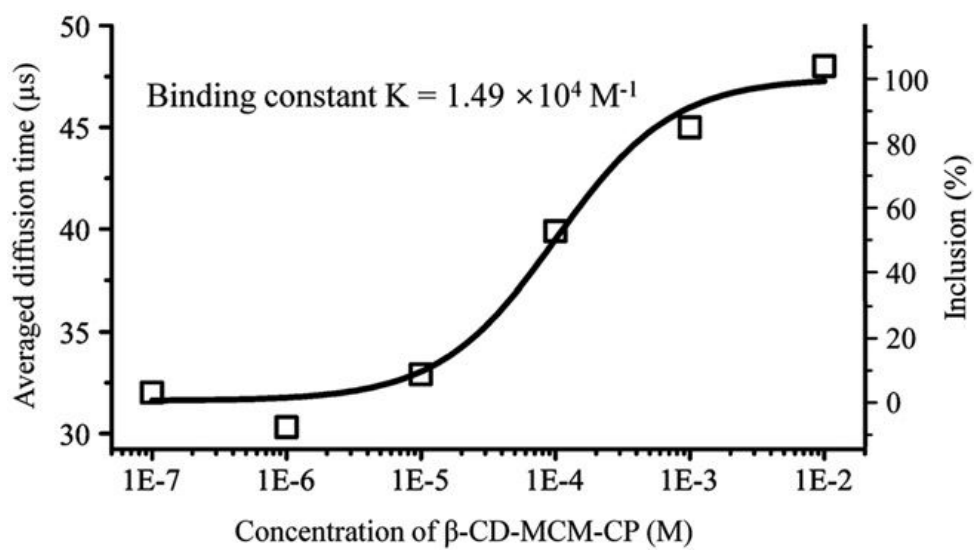


Figure 7. Variation of the average diffusion time measured by FCS to confirm the complex formation between β -CD-MCM-CP and FITC-hex-ADM.

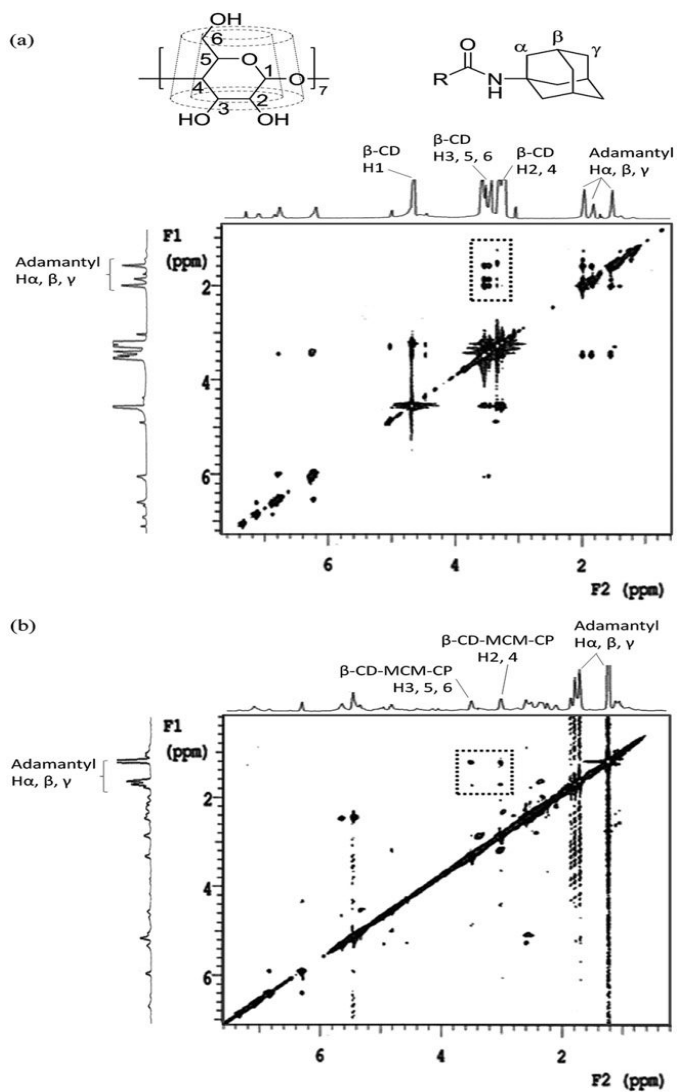


Figure 8. Expansion of NMR 2D ROESY (NMR solvent: D₂O) spectra of the inclusion complex between (a) β-CD and FITC-hex-ADM and (b) β-CD-MCM-CP and FITC-hex-ADM.

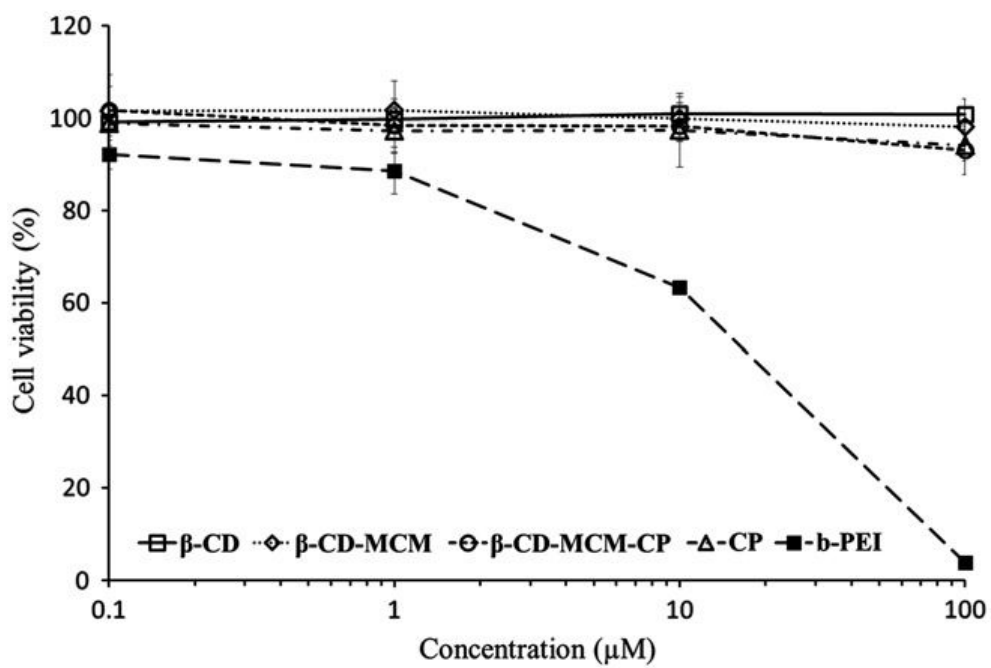


Figure 9. Cytotoxicity in NIH3T3 cells of β -CD (□), β -CD-MCM (◇), β -CD-MCM-CP (○), CP (△) and PEI (■). Each error bar represents the standard deviation (n=3).

국문 초록

우리는 β -사이클로덱스트린과 말레산 무수물에 기반한 pH에 민감한 약물 전달 운반체를 개발했다. β -사이클로덱스트린의 1차 OH작용기와 말레산 무수물의 잔기가 성공적으로 결합을 이루어서 메두사 형태와 같은 β -cd-mcm 을 형성했다. MCM 잔기는 세프라딘 약물과 높은 효율로 (490%) 결합을 형성했다. 더욱이 주목할 만한 것은 β cd-mcm-cp는 pH가 7.4에서 5.5로 떨어지는 작은 변화에서도 80% 이상의 약물이 30분만에 떨어지는 것을 보여 주었다는 것이다. 아다만탄 파생물은 β -cd-mcm-cp와 간단히 섞어주는 것만으로도 β -사이클로덱스트린의 안의 공간으로 삽입되는 것을 알 수있는데 이러한 사실을 통하여 다양한 작용기들을 도입할 수 있다. 이러한 다양한 장점들을 통해 β cd-mcm은 약산성인 조직이나 장기, 예를 들면 암세포나 감염조직, 농양, 엔도솜을 목표로 약물을 전달 할 수 있다. 그리고 아다만탄 끝에 특정 성질을 가진 물질, 예를 들면 리간드나 세포 투과성 물질을 쉽게 붙이는 것이 가능해서 더욱더 효과적인 약물전달체가 될 수 있을 것으로 예상된다.

주요어: 세프라딘, 약물 전달, 말레산 무수물, 아다만탄, 사이클로덱스트린

학번: 2012-20274